Atmospheric Environment 120 (2015) 76–88

Contents lists available at ScienceDirect

Atmospheric Environment

journal homepage: www.elsevier.com/locate/atmosenv

Probing the severe haze pollution in three typical regions of China: Characteristics, sources and regional impacts

Qiongzhen Wang [a, d], Guoshun Zhuang [a, *], Kan Huang [b, **], Tingna Liu [a], Congrui Deng [a], Jian Xu [a], Yanfen Lin [c], Zhigang Guo [a], Ying Chen [a], Qingyan Fu [c], Joshua S. Fu [b], Jiakuan Chen [d]

[a] Center for Atmospheric Chemistry Study, Department of Environmental Science and Engineering, Fudan University, Shanghai, 200433, PR China
[b] Department of Civil and Environmental Engineering, University of Tennessee, Knoxville, TN, 37996, USA
[c] Shanghai Environmental Monitoring Center, Shanghai, 200030, PR China
[d] School of Life Sciences, Fudan University, Shanghai, 200433, PR China

HIGHLIGHTS

- Contrasting characteristics of aerosol at three regions in a severe haze event.
- First observation of aerosol over East China Sea impacted by inland emissions.
- Important role of vehicular emission in triggering the heavy haze.

ARTICLE INFO

Article history:
Received 22 February 2015
Received in revised form
12 August 2015
Accepted 25 August 2015
Available online 28 August 2015

Keywords:
Haze
Sources
Formation process
Regional transport

ABSTRACT

$PM_{2.5}$ with its major chemical components were measured and analyzed during a concurrent haze in Jan. 1–19, 2013 at three sites (Shanghai, Beijing, and Huaniao, a remote isle over the East China Sea) to probe the sources and formation process of such a severe haze over three typical regions in China. The mean $PM_{2.5}$ concentrations during the severely polluted days reached 180.8 μg m^{-3}, 299.2 μg m^{-3}, and 131.1 μg m^{-3} in Shanghai, Beijing, and the Huaniao Isle, respectively. The mass ratio of the sum of SO_4^{2-}, NO_3^-, and NH_4^+ to $PM_{2.5}$ were over 1/3 during the polluted days at all the three sites. Promoted gas-to-particle transformations from acidic SO_2 and NO_x to SO_4^{2-} and NO_3^- under high relative humidity conditions played a major role in the formation of this severe haze. Significant contribution of traffic emissions to the haze formation over China was suggested to be one of the major sources in triggering the heavy haze over China. Specifically, there was a more contribution from traffic in Shanghai than in Beijing as indicated by the higher NO_3^-/SO_4^{2-} ratio in Shanghai. In Beijing, the enhanced coal combustion for winter heating along with the traffic emission was suggested to be the major two sources of this haze episode. Typical pollution elements such as As, Cd, and Pb as well as Cl^- and K^+ were substantially enhanced in the severely polluted days. Although the Huaniao Isle is located in the remote oceanic area as a background site, pollution elements, secondary ions, and K^+ all increased substantially during the polluted days. As visualized by the backward air mass trajectories associated with the potential source region identification technique, air masses that passed over Northern China and Yangtze River Delta evidently invaded the offshore areas of Eastern China. The ratios of As, Cd, Cu, Zn, and K^+ to Al at the Huaniao Isle were closer to those of Beijing rather than Shanghai, indicating that the marine aerosol over the East China Sea had been significantly polluted via the long-range transport of anthropogenic pollutants originating from Northern China.

1. Introduction

Haze, mostly caused by high concentrations of fine particles in atmosphere, has attracted worldwide attention in recent years due

* Corresponding author.
** Corresponding author.
E-mail addresses: gzhuang@fudan.edu.cn (G. Zhuang), khuang7@utk.edu (K. Huang).

http://dx.doi.org/10.1016/j.atmosenv.2015.08.076
1352-2310/

to its adverse effects on visibility (Chen et al., 2003), public health (Zhang et al., 2014b), and climate change (Menon et al., 2002). Due to the rapid economic development, urbanization, and motorization, haze frequently occurred in China during the past decade, especially in those densely populated regions such as the Beijing–Tianjin–Hebei region (BTH), the Yangtze River Delta (YRD), and the Pearl River Delta (PRD). Since January 2013, several severe haze episodes occurred over Northern and Eastern China. $PM_{2.5}$ concentrations in these episodes were in hazardous levels that directly threatened transportation and public health. Thus, it should be urgent to understand the sources and formation mechanisms of haze and assess its impacts on human health and climate change for the purpose of sound emissions control strategies.

Haze is closely related to the large emissions of sulfur dioxide (SO_2), nitrogen oxides (NO_x), volatile organic compounds (VOCs), and particulate matter (PM) from anthropogenic activities such as industries, traffic transportation, power plants, and biomass burning. In China, coal is the dominant fuel used for energy production, and coal combustion is the major source of SO_2 emissions. Meanwhile, the rapid increase of motor vehicles has become a more and more significant contributor to the NO_x and PM emissions in urban areas (Lang et al., 2012). The dominant sources and formation mechanisms of haze vary among different seasons. The open burning of biomass contributes significantly to the haze pollution during the post-harvest seasons, i.e., May–June and October–November (Cheng et al., 2014; Huang et al., 2012), while coal combustion plays a major role in the formation of haze in winter, particularly in those areas where coal is largely used for heating (Sun et al., 2013b; Zhao et al., 2013b). The gas-to-particle transformation of those pollution gases SO_2, NO_x, and VOCs is another major factor influencing the formation of haze. During haze episodes, secondary components NO_3^-, SO_4^{2-}, NH_4^+ together with organic matter always substantially increase (Zhao et al., 2013c), and become the most abundant components in aerosols (Kang et al., 2004; Tan et al., 2009). The sum of NO_3^-, SO_4^{2-}, and NH_4^+ can even account for 77% of the total $PM_{2.5}$ mass during haze days (Huang et al., 2012). Over the North China Plain, it is found that the reaction of photo-excited NO_2^* with water vapor, the NO_2 heterogeneous reactions on aerosol surfaces, and direct emissions of nitrous acid (HONO) play an important role in the formation of NO_3^- and NH_4^+ (An et al., 2013) and visibility degradation (Li et al., 2014). Heterogeneous chemical processing could change the oxidizing capacity of the atmosphere, aerosol chemical composition as well as optical properties (Zhu et al., 2010). In addition, unfavorable meteorological conditions can easily trigger the formation of haze (Meng et al., 2000; Sun et al., 2006). Haze frequently occurs under stagnant weather conditions where atmospheric pollutants are trapped and substantially increased (Zhang et al., 2014a; Zhao et al., 2013c). Meanwhile, high relative humidity favors the gas-to-particle transformation of pollution gases (Sun et al., 2013a), which contributes significantly to haze pollution.

Haze pollution is not a local environmental issue. Both local emission and regional transport contribute to haze formation. Due to the East Asian monsoon, air pollutants can be transported far away and impact greatly on the air quality of those downstream areas (Hsu et al., 2009). Along with the regional transport of air pollutants, haze pollution can be geographically extended even to those areas with few local pollution emissions (Zhao et al., 2013c).

In January 2013, an extremely severe haze shrouded over northern and eastern China, which lasted for about a week from Jan. 9 to 16. During this episode, the hourly $PM_{2.5}$ concentrations in many cities much exceeded the upper limit of the Air Quality Index, and the visibility was extremely low that caused cancellation of flights (http://www.theguardian.com/world/2013/feb/16/chinese-struggle-through-airpocalypse-smog). This severe haze pollution has attracted great attentions of the public, government, and atmospheric researchers in China. Zhang et al. (2014a) studied the meteorological conditions during this haze pollution, and the results showed that a weak East Asian winter monsoon existed in January and the weakened surface winds favored the formation of fog and haze in eastern China. Based on an intensive aerosol and trace gases observation at eleven sites, Wang et al. (2014c) identified this haze episode over BTH. The quick transformation of pollution gases to aerosols was suggested to be the internal cause of this severe haze pollution. In Beijing, high sulfur and nitrogen oxidation ratios were found, further indicating that the secondary transformation was a major contributor to the haze formation (Ji et al., 2014). With ACSM (Aerosol Chemical Speciation Monitor) observation, Sun et al. (2014) investigated the sources and chemical evolution of this haze over Beijing, and the results showed coal combustion was the largest source of primary organic aerosol (OA), which on average accounted for 20–32% of OA, and regional transport contributed significantly to the formation of this haze. Model simulation also indicated that regional transport played an important role in the formation of this regional haze over BTH (Wang et al., 2014b, 2014d). During Jan. 14–16, 2013, about 25% of the elemental carbon particles in Nanjing were from the regional transport (Wang et al., 2014a).

Most studies related to this notorious haze focused on one specific site, e.g. Beijing. However, this haze was evidently not a local phenomenon but had much more profound influences in a widespread regional scale that the coverage of this haze reached over 1.4 million km^2 of China's territory. The extent of the regional impacts of such a haze and how this severe haze could impact on such a wide region has been rarely reported. In this regard, we investigate this notorious haze that hovered over a large geographic region at three monitoring sites, including two urban sites, i.e. Beijing, Shanghai, and a remote site over the East China Sea, the Huaniao Isle. $PM_{2.5}$ with its major chemical components were measured and analyzed during this concurrent severe haze in Jan. 1–19, 2013 synchronously at these three sites to reveal the source and formation process of such a severe haze in the three typical regions in China. In particular, the relative contributions of stationary vs. mobile sources and regional transport of air pollutants were explored.

2. Method

2.1. Field observation

$PM_{2.5}$ samples were collected in Shanghai (a representative site of the Yangtze River Delta region), Beijing (a representative site of the Beijing–Tianjin–Hebei region), and the Huaniao Isle over the East China Sea (a representative site of the remote areas over the ocean) during Jan. 1–19, 2013. The locations and the detailed information of the three sampling sites are marked in Fig. 1 and presented in Table 1. Aerosol samples were collected for 24 h (normally from 10:00 AM to 10:00 AM of the next day) on Whatman 41 filters (Whatman Inc., Maidstone, UK) by medium-volume samplers (Qingdao Hengyuan Science &Technology Development Co., Ltd.; model: HY-100 $PM_{2.5}$; flow rate: 100 l min^{-1}). More samples were collected in those severe haze days. All the samples were put in polyethylene plastic bags immediately after sampling and then reserved in a refrigerator. All the filters were weighed before and after sampling using an analytical balance (model: Sartorius 2004 MP; reading precision: 10 μg) after stabilizing under constant temperature (20 ± 1 °C) and humidity (40 ± 2%) in a chamber for over 48 h. All the procedures were strictly quality controlled to avoid the possible contamination of the samples.

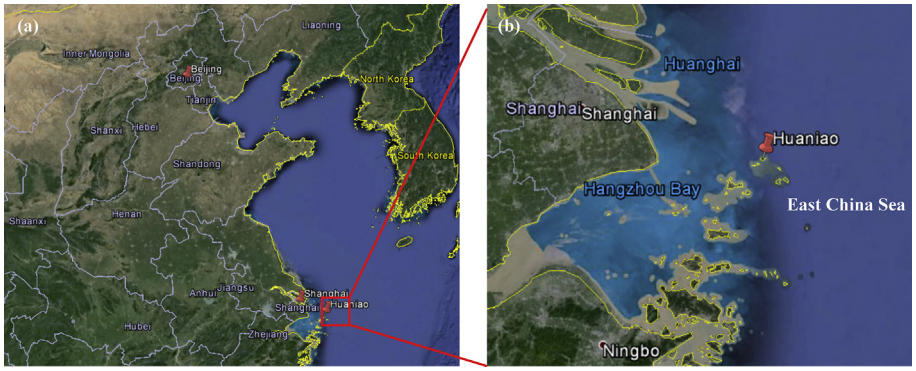

Fig. 1. (a) Locations of the three sampling sites (Beijing, Shanghai and the Huaniao isle) in this study (b) the enlarged map showing the location of the Huaniao isle over the East China Sea (the background map is from Google Earth).

2.2. Chemical analysis

2.2.1. Ion analysis

One fourth of each aerosol sample and the blank filter were extracted ultrasonically by 20 ml deionized water (18 MΩ cm^{-1}). Inorganic ions Na^+, NH_4^+, K^+, Mg^{2+}, Ca^{2+}, SO_4^{2-}, NO_3^-, and Cl^- were analyzed by an Ion Chromatography (IC; Dionex ICS 3000, USA) with separation columns of Dionex Ionpac AS 11 for anion and Dionex Ionpac CS 12A for cation as well as guard columns, a self-regenerating suppressed conductivity detector of Dionex Ionpac ED50, and a gradient pump of Dionex Ionpac GP50. The procedures were described in detail by Yuan et al. (2003).

2.2.2. Element analysis

Half of each aerosol sample and the blank filters were digested at 180 °C for 30 min in a high pressure Teflon digestion vessel with 8 ml concentrated HNO_3, and 0.6 ml concentrated HF by a Microwave Accelerated Reaction System (MARS 5; CEM, USA). The solutions were dried, and then diluted to 10 ml with 0.2 ml concentrated HNO_3 and deionized water (18 MΩ cm^{-1}). Total 13 elements (Al, Fe, Mn, Ti, Ni, Cu, P, Pb, Zn, Cd, V, Sr, and As) were measured by an inductively coupled plasma optical emission spectroscopy (ICP-OES; SPECTRO, Germany). The detailed analytical procedures were given elsewhere (Guo et al., 2014).

2.3. Daily PM_{10} and meteorological data

Air pollution index (API) data in 120 cities over China were downloaded from the data center of Ministry of Environmental Protection of China (http://datacenter.mep.gov.cn/). API was then converted to PM_{10} concentration according to the following formula:

$$C = C_{low} + \left[(I - I_{low}) \Big/ \left(I_{high} - I_{low}\right)\right] \times \left(C_{high} - C_{low}\right),$$

where C is the concentration of PM_{10} and I is the API value of PM_{10}; I_{high} and I_{low}, the two values that the most approaching to value I in the API grading limited value table, stand for the value larger and lower than I, respectively; C_{high} and C_{low} represent the PM_{10} concentration corresponding to I_{high} and I_{low}, respectively.

The meteorological data, including wind speed, wind direction, etc., were obtained from the National Climatic Data Center (NCDC).

3. Results and discussion

3.1. Regional occurrence of severe haze

Fig. 2 depicts the spatiotemporal variation of an extremely severe haze episode as indicated by the daily PM_{10} concentrations over 120 Chinese cities during Jan. 9–17, 2013. The spatial pattern of PM_{10} showed that the most severe pollution occurred over Northern China, including Beijing, Tianjin, Hebei, Henan, and Shandong provinces. During Jan. 9–14, the PM_{10} concentrations in the cities of Beijing, Tianjin, Baoding, Tangshan, Shijiazhuang, and Handan were mostly higher than 500 μg m^{-3}, or even up to 600 μg m^{-3} (the highest concentration recorded by the API of PM_{10}) at some areas. It was reported that the hourly $PM_{2.5}$ concentrations in Beijing even reached over 900 μg m^{-3} during this episode (http://cleanairinitiative.org/portal/node/11599; http://www.chinadaily.com.cn/hqpl/zggc/2013-01-14/content_8024128.html). The air quality in Northern China was crazy bad during this period. In central China regions, such as Anhui, Hunan, and Hubei provinces, PM_{10} concentrations with daily values of more than 150 μg m^{-3} were observed during Jan. 9–14, while even higher of more than 200 μg m^{-3} during Jan. 10–15. This high pollution stretched southward to YRD, where daily PM_{10} concentrations were mostly higher than 150 μg m^{-3} during Jan. 12–16. In Shanghai, the hourly $PM_{2.5}$ concentrations frequently exceeded 200 μg m^{-3} and daily $PM_{2.5}$ in Hangzhou ranged from 170 to 200 μg m^{-3} on Jan. 12, 13, and 15, indicating the concurrent severe air pollution over YRD. Overall, more than 17 provinces were influenced by this severe air pollution, covering a widespread territory of China with more than 1.4 million km^2. In the following discussions, the characteristics of $PM_{2.5}$ in the three representative sites, i.e. Beijing in Northern

Table 1
Detailed information of the three sampling sites.

Site	Site description
Beijing (BJ) (39°54′ N,116°24′ E)	Urban site; residential, traffic; Aerosol samples were collected on the roof of a 20 m-tall teaching building in Beijing University of Technology.
Shanghai (SH) (31°18′ N, 121°30′ E)	Urban site; residential, traffic; Aerosol samples were collected on the roof of a 20 m-tall teaching building in Fudan University.
Huaniao Isle (HN) (30°51′ N,122°40′ E)	Remote site with a total population of 2431 and a land area of 3.28 km^2; Aerosol samples were collected on the roof of a 16 m-tall lighthouse.

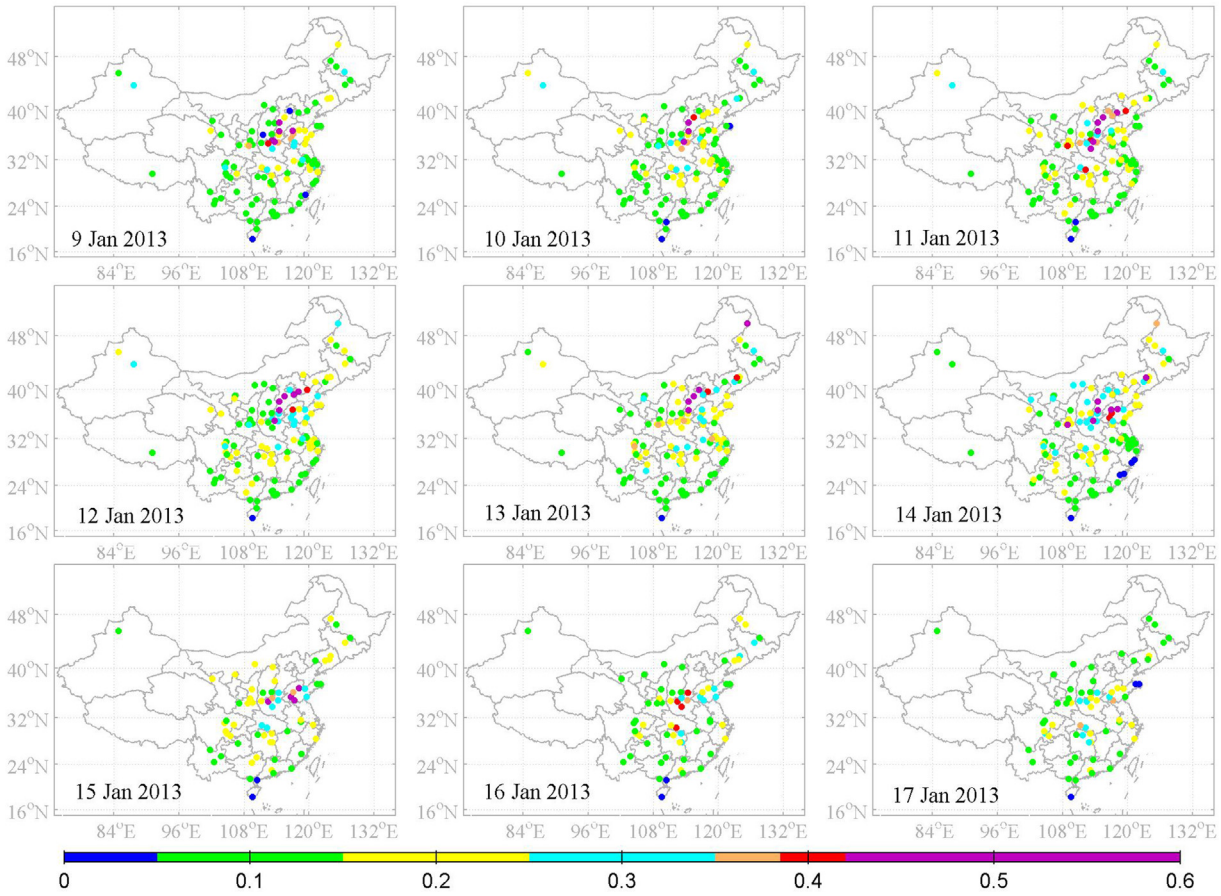

Fig. 2. PM_{10} concentration (mg m^{-3}) in 120 cities over China during Jan. 9–17 (PM_{10} concentration and the corresponding air pollution level are presented in color. Blue, green, yellow, cyan, khaki, red, and purple present excellent, good, slightly polluted, lightly polluted, moderately polluted, heavily polluted, and severely polluted day, respectively, when the PM_{10} concentrations are in the range of 0–0.05 mg m^{-3}, 0.05–0.15 mg m^{-3}, 0.15–0.25 mg m^{-3}, 0.15–0.35 mg m^{-3}, 0.35–0.385 mg m^{-3}, 0.385–0.42 mg m^{-3}, >0.42 mg m^{-3}, according to the air pollution index.). (For interpretation of the references to color in this figure caption, the reader is referred to the web version of this article.)

China, Shanghai in Eastern China, and a remote site, the Huaniao Isle over the East China Sea, were analyzed to reveal the sources and formation processes of this severe episode.

Fig. 3 shows the time series of daily $PM_{2.5}$ and major meteorological parameters from Jan. 1–19 in Shanghai (SH), Beijing (BJ), and the Huaniao Isle (HN), respectively. According to the Chinese National Air Quality Standards II (the daily average of 75 μg m^{-3} is the threshold), daily $PM_{2.5}$ concentrations lower than 75 μg m^{-3} were regarded as normal days (ND), i.e. Jan. 3–10 (excluding the rainy days on Jan. 6–7) in Shanghai (ND_SH), Jan. 1–5 in Beijing (ND_BJ), and Jan. 1–11 (excluding the rainy days on Jan 6–7 and 9) at the Huaniao Isle (ND_HN). In Shanghai, Jan. 12–15 was identified as the most severe air pollution days (PD_SH), when the visibility was mostly below 5 km with the mean $PM_{2.5}$ concentration of as high as 180.8 μg m^{-3} (Fig. 3a), more than twice of Chinese National Air Quality Standards II. On the first day of SH_PD (Jan. 12), weak wind (2.0 ± 1.0 m s^{-1}) was observed and $PM_{2.5}$ concentration reached 201.2 μg m^{-3}. On Jan. 14 when the wind speed increased to 3.1 ± 1.3 m s^{-1}, $PM_{2.5}$ showed a corresponding drop to 129.1 μg m^{-3}. During these days, winds mainly prevailed from the north, northwest and northeast. On Jan. 16 when the wind direction changed from the south with increased wind speed of 4.8 ± 0.7 m s^{-1}, hourly $PM_{2.5}$ increased again to be higher than 200 μg m^{-3}, implying different sources for haze among the days during PD_SH. Overall, the mean relative humidity, wind speed, and mixing height during PD_SH reached 79.9%, 3.0 m s^{-1}, and 386 m, indicating more unfavorable synoptic condition as compared to those of 70.1%, 3.8 m s^{-1}, and 652 m during ND_SH.

In Beijing (Fig. 3b), the wind speed decreased from 4.4 ± 2.3 m s^{-1} on Jan. 8 to 2.1 ± 1.2 m s^{-1} on Jan. 9, correspondingly the $PM_{2.5}$ concentration increased from 40.1 μg m^{-3} to 92.7 μg m^{-3}. In the meantime, wind direction changed from north and northeast to southwest, potentially bringing air pollutants from Beijing's neighboring Hebei province, which had been highly polluted due to intense local industrial activities (Wang et al., 2014d). On the early morning of Jan. 10, visibility rapidly degraded to be lower than 5 km (mostly lower than 2 km) with greatly enhanced humidity. Accordingly, the $PM_{2.5}$ concentration sharply increased to be 286.9 μg m^{-3}, and stayed at high concentrations of more than 200 μg m^{-3} until Jan. 13, with a maximum of 413.0 μg m^{-3} on Jan. 12. Jan. 10–13 was identified as the most severely polluted days in Beijing (PD_BJ). During this period, the mean mixing layer height was only 133 m with high relative humidity of 77.6%, which was attributed to the frequent occurrences of fog events (Sun et al., 2014; Huang et al., 2014). The mean $PM_{2.5}$ concentration during PD_BJ reached 299.2 μg m^{-3}, which was about 7 times of that during ND_BJ (43.3 μg m^{-3}), and more than 8 times of U.S. EPA daily standard (35 μg m^{-3}) and 4 times of Chinese National Air Quality Standards II, revealing the air quality was extremely severe during this period.

Compared to the severe air pollution of these mega-cities, the Huaniao Isle evidently showed much better air quality considering

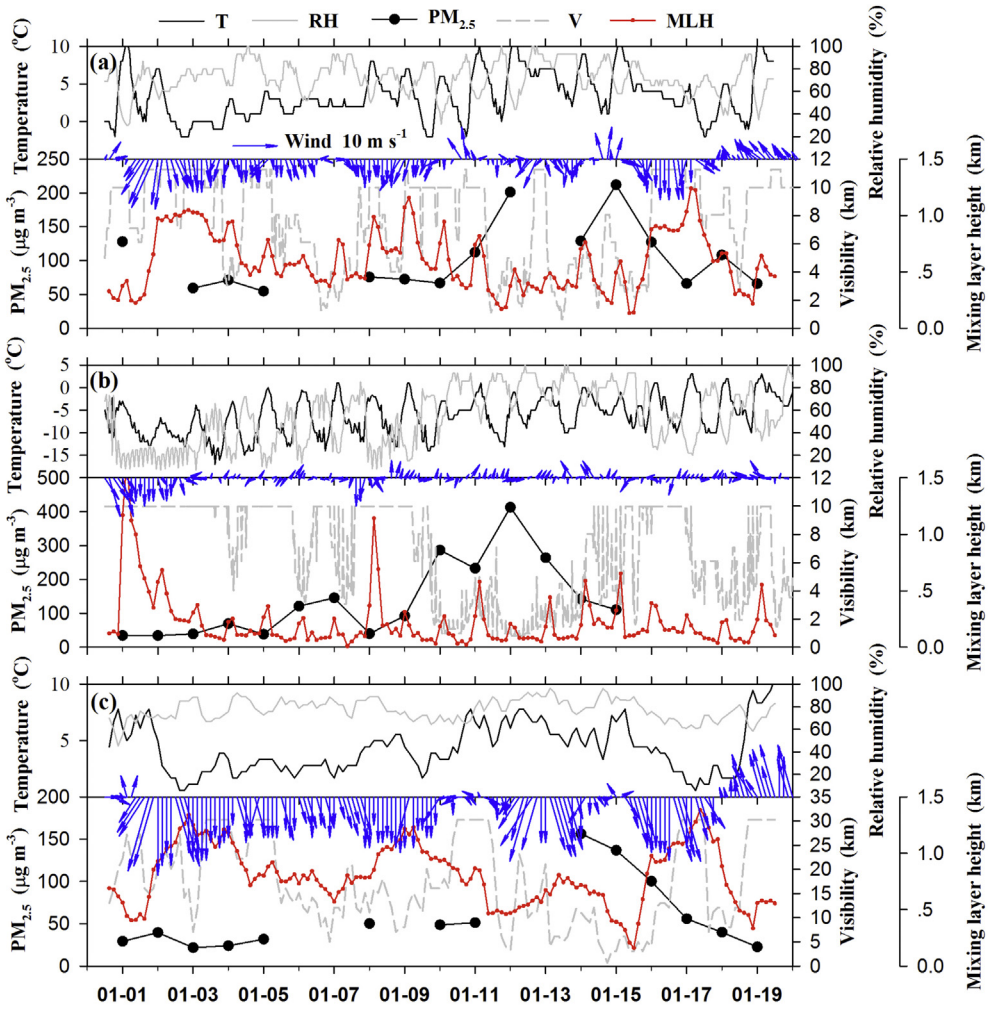

Fig. 3. Time series of $PM_{2.5}$ daily concentration, hourly ambient temperature, relative humidity, wind speed/direction, visibility and 3-hourly mixing layer height (computed from the NCEP Global Data Assimilation System (GDAS) model, http://ready.arl.noaa.gov/READYamet.php) in (a) Shanghai, (b) Beijing, and (c) the Huaniao Isle during Jan. 1–19 (the missing $PM_{2.5}$ data is due to raining or the maintenance of samplers).

the fact that there were negligible local emission sources there. Wind speeds were obviously higher of 4.2 ± 1.5 m s^{-1} and the wind direction was dominantly from the north (Fig. 3c). However, within the same period of the heavy air pollution as Shanghai on Jan. 14–16 (PD_HN), the mean $PM_{2.5}$ concentration at the Huaniao Isle still reached to be 131.1 μg m^{-3} with the lowest visibility of 3 km during the whole study period. This indicated that even the remote areas could not be exempted from this widespread haze pollution.

3.2. Chemical evolution and sources of the haze at three typical sites

3.2.1. Shanghai

Fig. 4a shows the time-series of major water-soluble ions in Shanghai. The sum of all ions measured substantially increased during PD_SH, which, on average, accounted for 45% of $PM_{2.5}$, compared to that of 39% during ND_SH. As the most abundant ions, SO_4^{2-}, NO_3^-, and NH_4^+ increased substantially from 9.2, 9.2, and 4.9 μg m^{-3} during ND_SH to 25.7, 37.3, and 14.8 μg m^{-3} during PD_SH, respectively. As a result, the mass ratio of the sum of SO_4^{2-}, NO_3^-, and NH_4^+ (SNA) to $PM_{2.5}$ increased from 35% during ND_SH to 43% during PD_SH. The concentration of NO_3^- was comparable to that of SO_4^{2-} during ND_SH, while during PD_SH NO_3^- even exceeded SO_4^{2-}. The mass ratios of PD_SH versus ND_SH for SO_4^{2-}, NO_3^-, and NH_4^+ were around 3, 5, and 3, respectively, indicating NO_3^- enhanced the most among the three species during the polluted days. The significant increase of NO_3^- probably suggested that the NO_x emissions increased the most as compared to other pollutants under the same synoptic system. Fig. S1 shows the daily mass ratio of NO_2/SO_2 for the whole Shanghai city during the study period. It is clearly shown that during the pollution episode (Jan. 11–15) in Shanghai, the NO_2/SO_2 ratios (except for Jan. 12) were much higher than the other days. The average NO_2/SO_2 ratio during the pollution episode reached 2.9 compared to that of 1.7 during the other days. Power plants and industries were emission sources for both SO_2 and NO_2. If the pollution episode was mainly caused by either of these two emission sectors or both of them, the increases of emission rates of power plants and industries shouldn't greatly change the ratios of NO_2/SO_2, i.e. should be as similar as those non-polluted days. However, the enhanced NO_2/SO_2 ratios during the polluted episode indicated an evident perturbation from other emission sources. As the transportation emission sector is the major source for NO_x but not for SO_2, we think the more increase of NO_3^- than SO_4^{2-} should be partly due to the enhanced contribution from the transportation sector to the total NO_x emissions. As the residential winter heating facilities were rarely built in Southern China, the emission from coal combustion in winter should not have much difference compared to that in other seasons, and, in

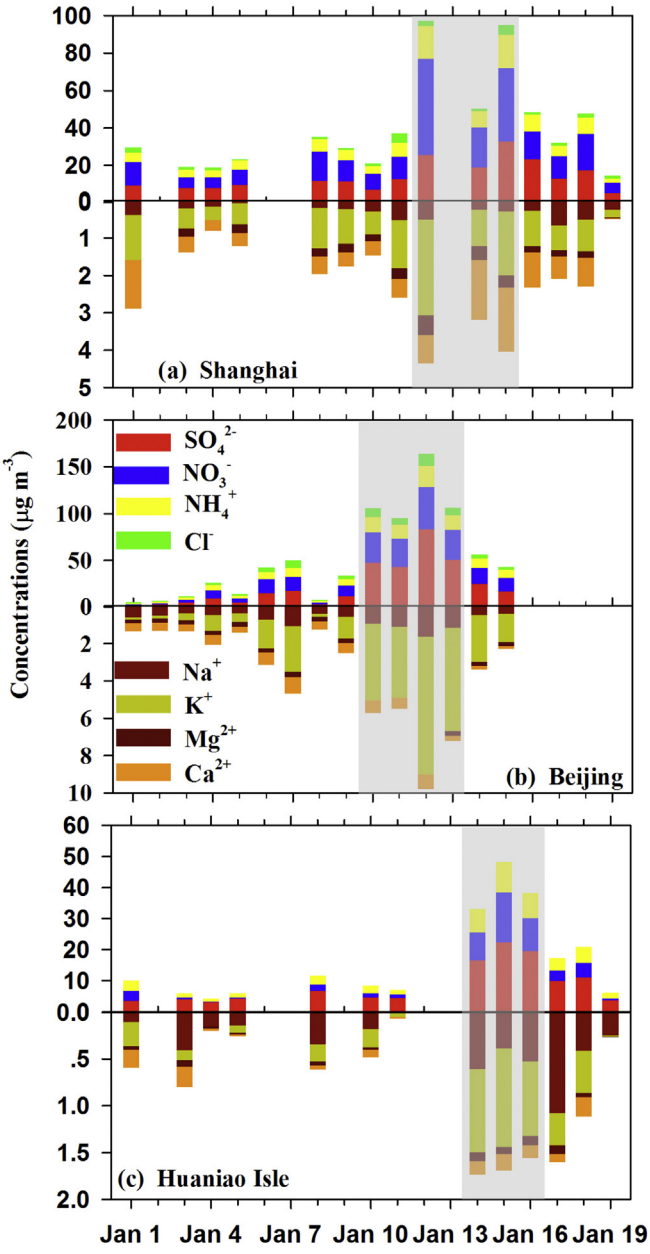

Fig. 4. Time-series of major water-soluble ions in $PM_{2.5}$ in (a) Shanghai, (b) Beijing, and (c) the Huaniao Isle.

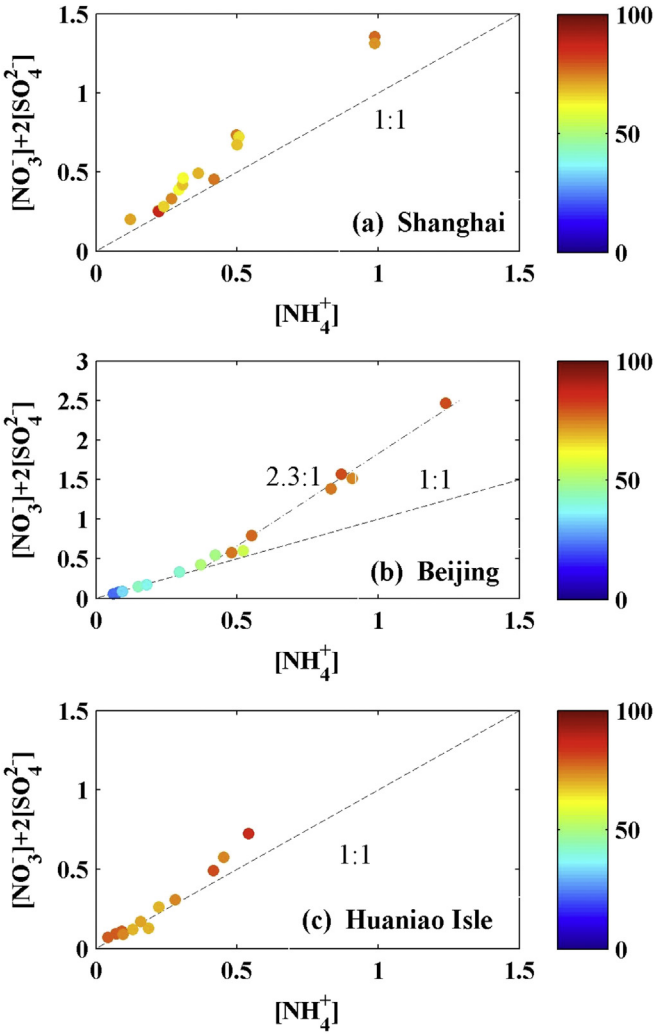

Fig. 5. Relationship between NH_4^+ (neq m^{-3}) and the sum of SO_4^{2-} and NO_3^- (neq m^{-3}) in (a) Shanghai, (b) Beijing, and (c) the Huaniao Isle, respectively. All the scatters are color coded by relative humidity (RH, %). The 1:1 line is plotted in the figure as reference. (For interpretation of the references to color in this figure caption, the reader is referred to the web version of this article.)

turn, the significant increase of NO_3^- was more ascribed to vehicle emission. Compared to NO_3^-, the increases of non-sea-salt (nss) Cl^- and K^+ during PD_SH, which were estimated based on the assumption that all Na^+ was from the marine source using the marine equivalent Cl^-/Na^+ ratio of 1.17 and K^+/Na^+ ratio of 0.022, were moderate of about 2-folds. Particulate Cl^- was mostly associated with coal combustion in winter (Yao et al., 2002). K^+ was regarded as a typical tracer for aerosols emitted from biomass burning (Andreae, 1983), however, it could also be enriched in the particles from coal combustion (Hsu et al., 2009; Takuwa et al., 2006). The characteristics of both Cl^- and K^+ indicated that the contributions from either biofuels usage or coal combustion to the haze were less significant than traffic emission in Shanghai. As for Ca^{2+} during the severe haze episode, it was enhanced about 3.6 folds in Shanghai than that of 1.4 folds in Beijing which will be discussed below, implying that the role of traffic emission in the haze formation was more prominent in Shanghai since a considerable part of Ca^{2+} derived from the re-suspended road dust due to traffic running in the urban sites.

The equivalent ratio of anions to cations measured in Shanghai, i.e. $([NO_3^-]+2[SO_4^{2-}]+[Cl^-])$ to $([NH_4^+]+[Na^+]+[K^+]+2[Mg^{2+}]+2[Ca^{2+}])$, ranged from 1.1 to 1.3 during the whole study period, revealing that Shanghai was in the ammonium-poor environment in winter and the aerosols were weakly acidic. The relative humidity (RH) during the whole study period was overall above 60%, suggesting the aqueous-phase chemical processing should be ubiquitous during both ND_SH and PD_SH days. Fig. 5 shows the relationship between NH_4^+ and the sum of SO_4^{2-} and NO_3^- under different RH at the three sites. The units of all species are equivalent concentrations (μeq m^{-3}) and all the scatters are color coded by RH in Fig. 5. The ratio of $([NO_3^-]+2[SO_4^{2-}])/[NH_4^+]$ in Shanghai (Fig. 5a) did not show difference as distinct as in Beijing (Fig. 5b), which would suggest that the neutralization effect of NH_3 to the acids was similar between ND_SH and PD_SH days. This was mainly due to that the fluctuation of RH in Shanghai was not as strong as in Beijing. However, the ratio of $([NO_3^-]+2[SO_4^{2-}])/[NH_4^+]$ was lower in PD_SH than that in PD_BJ, which meant that the fraction of

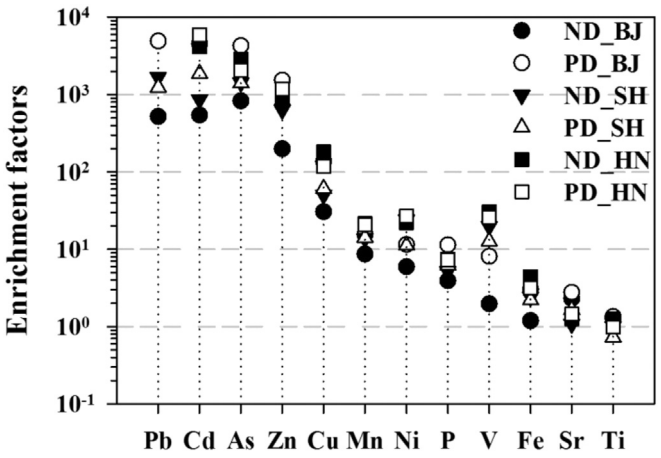

Fig. 6. Enrichment factors (EFs) of elements in normal days (ND) and in the severely polluted days (PD) in Shanghai (SH), Beijing (BJ), and the Huaniao Isle (HN).

those acidic components, e.g. HNO_3 and H_2SO_4, the oxidation products from NO_x and SO_2, neutralized by NH_3 was greater in Shanghai than in Beijing during the severe haze period. For SO_2 is mostly from coal combustion, less emission from coal combustion in winter in Shanghai than in Beijing should be mainly responsible for the lower ratio of $([NO_3^-] + 2[SO_4^{2-}])/[NH_4^+]$ in Shanghai.

Enrichment factors (EFs) of trace elements are good indicators pinpointing the extent of air pollutants accumulation as elements are almost all subject to primary emissions. EF is defined as $EF = (X/X_{Ref})_{aerosol}/(X/X_{Ref})_{crust}$, where $(X/X_{Ref})_{aerosol}$ and $(X/X_{Ref})_{crust}$ are the mass concentration ratios of an element interested, X, to a reference element, X_{Ref}, in aerosol and in crust (Lida, 2006), respectively. Al is the reference element used in this study. Fig. 6 shows the average EFs in the normal days (ND) and in the severely polluted days (PD). Those typical elements measured could be classified into two categories: 1) The EFs of Fe, Ti, and Sr were mostly lower than 5 during both ND and PD days at all the three sites. These elements, together with Al, were classified to be crustal elements. 2) The EFs of elements As, Cd, Cu, Mn, Ni, Pb, V, and Zn, were higher than 10, suggesting these elements were moderately or severely influenced by anthropogenic sources and these eight elements were classified to be pollution elements.

Fig. 7 shows the ratios of the mean concentrations of ions and elements in PD to those in ND, i.e. PD/ND. In Shanghai, the mean concentrations of pollution elements As, Cd, Cu, Mn, Pb, and Zn reached 21.0 ng m^{-3}, 2.1 ng m^{-3}, 31.3 ng m^{-3}, 0.1 μg m^{-3}, 0.2 μg m^{-3}, and 0.5 μg m^{-3} in PD_SH, 3–6 times of those in ND_SH (Fig. 7a). The EFs of As, Cd, Cu, Pb, and Zn also increased to 50–5000 (Fig. 6). Coal combustion was the major source of As, Cd, and Pb (Duan and Tan, 2013; Tian et al., 2012, 2010), while Zn and Cu were mostly associated with traffic emission (Tanner et al., 2008) and industrial emission (Cheng et al., 2012), and Mn was associated with metallurgical process (Sun et al., 2004). Thus, the enhancements of these pollution elements were indicative of emission sources from coal combustion, vehicles, and industries. The crustal elements, Al, Fe, Ti, and Sr, in Shanghai were also enhanced during

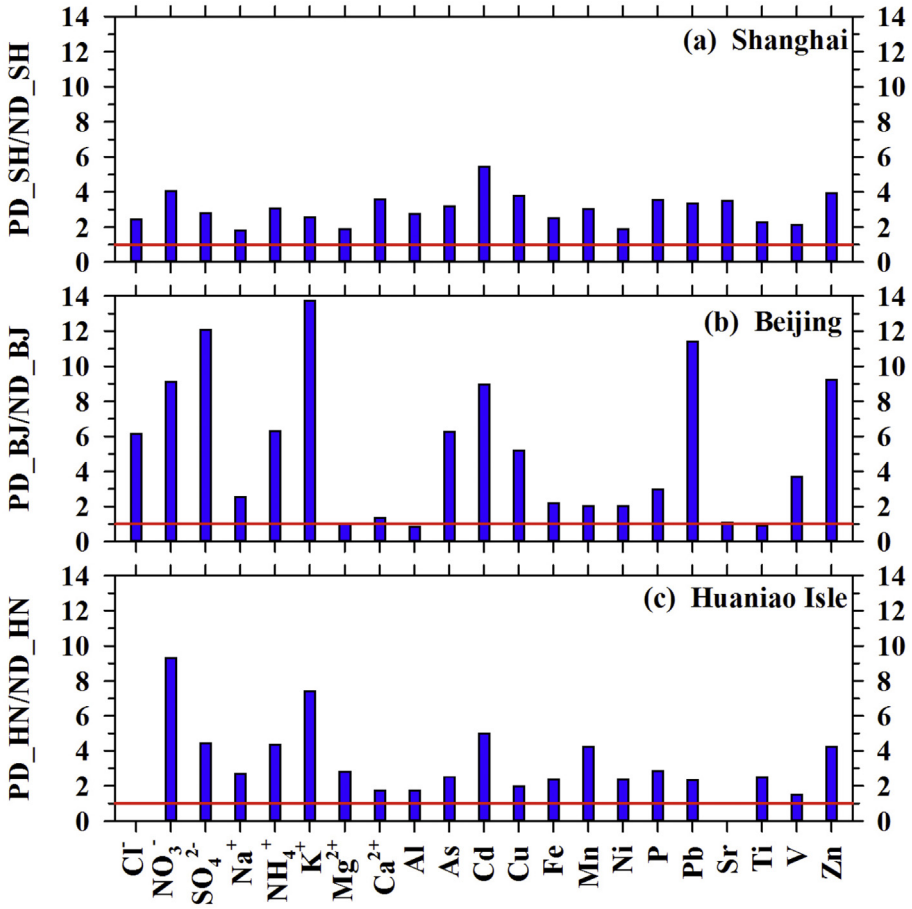

Fig. 7. Ratios of mean concentrations of ions and elements in the severely polluted days to those in normal days in (a) Shanghai, (b) Beijing, and (c) the Huaniao Isle.

those severely polluted days. This would further corroborate that the traffic emission was indeed a significant source as traffic activity could re-suspend the road dust and in turn increase the level of these crustal elements in the aerosols. Ni and V also increased in PD_SH with the moderate EFs of 10–25. It must be noted that the mean concentrations of Ni and V in PD_SH were 8.9 and 14.7 ng m^{-3}, even higher than those of 6.7 and 6.7 ng m^{-3} in PD_BJ. This was probably due to the contribution from the ship emission, as Ni and V were its typical tracers (Zhao et al., 2013a). The Shanghai Port has become the world's busiest container port since 2010 and ship emissions acted potentially as one of the major sources of the air pollution in Shanghai (Yang et al., 2007). The mass ratios of V/Ni were ~1.5 in both ND_SH and PD_SH, close to that (1.9) in heavy fuel oil used mostly in the domestic ships (Zhao et al., 2013a), suggesting the additional contribution from ship emissions to the haze over Shanghai.

3.2.2. Beijing

In Beijing, in consistent with the sharp increase of $PM_{2.5}$ during PD_BJ, the sum of all ions measured substantially increased to 125.0 μg m^{-3} on average, accounting for 42% of $PM_{2.5}$, compared to that of 14.3 μg m^{-3} during ND_BJ accounting for 31% of $PM_{2.5}$. In particular, secondary inorganic species SO_4^{2-}, NO_3^-, and NH_4^+ were significantly enhanced during PD_BJ (Fig. 4b) with mean concentrations of 56.1, 34.9, and 17.3 μg m^{-3}, respectively, about 12, 9, and 6 times of those during ND_BJ. In the meantime, the mass ratio of SNA to $PM_{2.5}$ also increased significantly from 24% during ND_BJ to 36% during PD_BJ. It was apparent that enhanced gas-to-particle transformation from SO_2 and NO_x to SO_4^{2-} and NO_3^- was one of the major causes of the extremely high $PM_{2.5}$ concentrations. As the most abundant species among SNA, SO_4^{2-} contributed about 50% to SNA and 19% to $PM_{2.5}$ during PD_BJ. Even during ND_BJ, SO_4^{2-} could contribute 44% to SNA and 10% to $PM_{2.5}$. Winter is the heating season in Northern China, thus, the enhanced coal combustion for residential heating was responsible for the high yields of SO_2 and NO_x. Significant increase of Cl^- was also observed from 1.5 μg m^{-3}, on average, during ND_BJ to 9.5 μg m^{-3} during PD_BJ, indicating that coal combustion played an important role in the haze formation during PD_BJ. It is noted that Cl^- in Beijing during PD_BJ was more than 3 times of nss-Cl^- in Shanghai during PD_SH (2.1 μg m^{-3}). In the meantime, the mass ratio of nss-Cl^- to $PM_{2.5}$ in Beijing reached ~4% during PD_BJ and ~3% during ND_BJ, much higher than that of ~1% in Shanghai. These were attributed to the larger coal consumption for residential heating in Northern China.

K^+ was also substantially enhanced during PD_BJ (Fig. 4b). The ratio of K^+ in PD_BJ to that in ND_BJ reached up to 14, even higher than the ratio of SNA between the two periods (Fig. 7b). K^+ reached 7.4 μg m^{-3} on Jan. 12, the highest daily concentration in the whole study period, which was comparable to the K^+ concentration in a pollution episode dominated by biomass burning (Huang et al., 2012). As mentioned above, particle K^+ was could be enriched in the particles either from biomass burning or coal combustion, thus the high K^+ concentrations during PD_BJ might be attributed to these two emission sources. The biofuels were widely used for residential cooking and heating in the rural areas of China (Mestl et al., 2007), thus biomass burning might be one of the sources of the severe haze in this period. However, due to the intense foggy weather (Sun et al., 2014; Huang et al., 2014), the fire spots caused by biomass burning couldn't be detected from the remote sensing technique in this case.

The equivalent ratios of $([NO_3^-] + 2[SO_4^{2-}])/[NH_4^+]$ were around 1.0 during ND_BJ (Fig. 5b), indicating sulfate and nitrate were almost fully neutralized by ammonium. During this period, RH was mostly below 50%. As RH was elevated to be above 70% with an average of (78 ± 3) % during PD_BJ, SO_4^{2-}, NO_3^-, and NH_4^+ were consistently enhanced as shown in Fig. 5b. However, the ratio of $([NO_3^-] + 2[SO_4^{2-}])/[NH_4^+]$ largely deviated away from the 1:1 line but substantially increased to 2.3 during PD_BJ, which indicated that in this severe haze episode sulfate and nitrate were far from fully neutralized due to the ammonium-poor environment in Beijing and the aerosol acidity could be much greater than in the normal days. The ratio of $([NO_3^-] + 2[SO_4^{2-}] + [Cl^-])/([NH_4^+] + [Na^+] + [K^+] + 2[Mg^{2+}] + 2[Ca^{2+}])$ during PD_BJ was calculated to be (1.7 ± 0.1), much greater than 1.0. This indicates that there was indeed a large deficit of cations, which should be attributed to the unmeasured hydrogen ions (H^+). High amounts of SO_2 and NO_x were emitted due to residential heating in winter in Northern China. In addition, this severe haze episode in Beijing was associated with abnormal high humidity (Zhang et al., 2014a), which could accelerate the aqueous-phase chemical process which was an effective pathway facilitating the transformation of SO_2 and NO_x, to be free acids, i.e. H_2SO_4 and HNO_3, via the H_2O_2/O_3 oxidation and metal catalysis (e.g. Fe^{3+} and Mn^{2+}) (Jacobson, 1997). By applying the E-AIM model (Extended Aerosol Thermodynamics Model, http://www.aim.env.uea.ac.uk/aim/aim.php) which considers a $H^+ - NH_4^+ - Na^+ - SO_4^{2-} - NO_3^- - Cl^- - H_2O$ system, aerosol LWC (Liquid Water Content) could be estimated based on the aerosol chemistry data measured in this study with the corresponding temperature and relative humidity. Fig. S2 shows the temporal variation of LWC and aerosol acidity (H^+_{Aer}). H^+_{Aer} is calculated from the difference between total equivalent concentrations of anions and that of cations: $[H^+_{Aer}] = 2[SO_4^{2-}] + [NO_3^-] + [Cl^-] - [NH_4^+] - [Na^+] - [K^+] - 2[Ca^{2+}] - 2[Mg^{2+}]$, the units of all ions are in molar concentrations (μmol/m^3). As shown in Fig. S2, LWCs were negligible before Jan. 10 due to that the daily RH values were mostly below 50%. The values of H^+_{Aer} were also relatively low and sometimes were zero (i.e. fully neutralized). In contrast, LWCs were significantly enhanced since Jan. 10. This would certainly promote the increase of SO_2 and NO_x uptake, as well as acceleration of the gas–liquid–solid reactions of SO_2 and NO_2 on particles, which could further lead to the increased hygroscopicity of particles. This was corroborated by the sharp increase of aerosol acidity as shown in Fig. S2 that H^+_{Aer} increased 2–10 times compared to the less polluted days. In this regard, we think the aqueous-phase reactions associated with enhanced LWC should have played an important role in promoting the formation sulfate and nitrate at elevated RH levels.

On the other hand, other meteorological parameters may also play crucial roles in the high yields of secondary aerosols. Fig. S3 shows the variations of hourly wind speed and temperature as a function of relative humidity (RH) during the whole study period in Beijing. All data are binned according to RH (10% increment). It is shown that temperature was relatively constant across different RH levels, while wind speed showed an evident decrease at higher RH levels. This probably indicated that the photochemistry was not the major driver influencing the formation of NO_3^- and SO_4^{2-} during this period. On the other hand, at higher RH, wind speeds were much lower than those at lower RH. The average wind speed at RH of 70–80%, 80–90%, and 90–100% was only 0.8, 0.6, and 0.6 m s^{-1}, respectively, much lower than those under the low RH conditions. It is well known that higher wind speed is especially efficient for cleansing the pollutants. This indicated that the atmospheric condition was very stagnant at higher RH, partly accounting for the high concentrations of NO_3^- and SO_4^{2-} during the polluted episode.

Finally, as the major neutralizer of acidic species, the NH_3 emission was at its lowest level as agricultural activities were mostly inactive in winter in Northern China. High yields of sulfate and nitrate far exceeded the amount that the ambient NH_3 could neutralize, resulting in a significant excess of free acids. Hence, the aerosols during this severe air pollution episode in Beijing were expected to be highly acidic.

As shown in Fig. 7b, the concentrations of the pollution elements significantly increased in PD_BJ compared to those in ND_BJ. For instance, the mean concentrations of As, Cd, Cu, Pb, and Zn were 54.8 ng m^{-3}, 4.8 ng m^{-3}, 57.7 ng m^{-3}, 0.5 μg m^{-3}, and 0.8 μg m^{-3} in PD_BJ, 5–13 times of those in ND_BJ, with the highest daily concentrations up to 88.9 ng m^{-3}, 6.5 ng m^{-3}, 88.7 ng m^{-3}, 0.7 μg m^{-3}, and 1.1 μg m^{-3} on Jan. 12, respectively. EFs of As, Cd, Pb, and Zn increased from 200–850 in ND_BJ to 1500–8000 in PD_BJ (Fig. 6), while EF of Cu increased from 31 to 136. Evidently, the pollution elements in PD_BJ were much more enriched in the severe haze days. As mentioned above, coal combustion was the major source of As, Cd, and Pb, the enhancement of these elements further suggested that the residential heating in winter was one of the causes of the highly enriched elements. While the enrichment of Zn and Cu in PD_BJ implied that traffic and industrial emissions were also two of the possible sources triggering the haze.

3.2.3. Huaniao Isle

The Huaniao Isle is the most eastward site over the East China Sea as shown in Fig.1b. During ND_HN, the mean concentrations of SO_4^{2-}, NO_3^-, and NH_4^+ were at low levels of 4.3, 1.3, and 1.9 μg m^{-3}, demonstrating the remote characteristics of this site. During PD_HN, significant increases of SO_4^{2-}, NO_3^-, and NH_4^+ were observed with mean concentrations of 19.5, 11.9, and 8.5 μg m^{-3}, respectively. Compared to ND_HN, these three species were enhanced over 4, 9, and 4 times, respectively. The enhanced folds were even higher than that in Shanghai. As a remote oceanic region where the local emissions were negligible, the abrupt increase of secondary aerosols provides strong evidence of invaded pollutants from long/medium-range transport. To exclude the contribution from marine source to SO_4^{2-} in the aerosols over the Huaniao Isle, nss $-$ SO_4^{2-} could be estimated based on the assumption that all Na^+ was from the marine source using the marine SO_4^{2-}/Na^+ ratio of 0.25. It was calculated that nss $-$ SO_4^{2-} accounted for 99% of the total SO_4^{2-} during both ND_HN and PD_HN, indicating that SO_4^{2-} of the Huaniao Isle was dominantly contributed by anthropogenic sources. This meant that the marine aerosol at the remote areas over the East China Sea was highly related to the regional and/or long-range transport. SNA accounted for 24% of $PM_{2.5}$ during ND_HN and 31% during PD_HN, respectively. The mass ratio of SNA to $PM_{2.5}$ at the Huaniao Isle was close to that in Beijing, a city far away from the isle, but much lower than that in Shanghai, the adjacent city to the isle, which suggested that the marine aerosol over the East China Sea was more influenced by the long-range transport (more discussion in Section 3.3). Also, the mean K^+ concentration increased from 0.1 μg m^{-3} in ND_HN to 0.9 μg m^{-3} in PD_HN, and the nss-K^+ accounted for ~96% of the total K^+ in both ND_HN and PD_HN, which indicated that K^+ at the Huaniao Isle was mostly from the regional/long-range transport of the anthropogenic emissions in the mainland China.

RH showed the highest values at the Huaniao Isle among the three sites, ranging from 69% to 86% during the study period and averaged (80 ± 14)% in PD_HN. The correlation between NH_4^+ and $([NO_3^-] + 2[SO_4^{2-}])$ as a function of RH was as similar as Shanghai while differed a lot from Beijing (Fig. 5c). During ND_HN, the ratio of $([NO_3^-] + 2[SO_4^{2-}])/[NH_4^+]$ was close to 1.0, indicating that sulfate and nitrate were almost fully neutralized by ammonium in the normal days at this isle. While during PD_HN, this ratio slightly increased to 1.3, indicating that the marine aerosol over this isle was weakly acidic and it was evidently from the regional/long-range transport of the anthropogenic emissions in the mainland of China.

EFs of the pollution elements at the Huaniao Isle were as high as those in Beijing and Shanghai (Fig. 6), indicating that the marine aerosol over this isle had evident anthropogenic origin. The mean concentrations of As, Cd, Cu, Mn, Pb, and Zn increased 2–5 folds from 3.0 ng m^{-3}, 0.4 ng m^{-3}, 7.5 ng m^{-3}, 9.9 ng m^{-3}, 3.1 ng m^{-3}, and 0.04 μg m^{-3} in ND_HN to 7.7 ng m^{-3}, 1.8 ng m^{-3}, 14.8 ng m^{-3}, 41.9 ng m^{-3}, 7.4 ng m^{-3}, and 0.2 μg m^{-3} in PD_HN, respectively. Specifically, EFs of Ni and V at the Huaniao Isle were the highest among all three sites (Fig. 6). As a remote site approximately 60 km away from a large and busy container port (Yangshan port), the significant enrichment of Ni and V was evidently due to the contribution from those busy ship activities over the Eastern China Sea (Lin et al., 2013). The mean ratio of V/Ni was ~2.2 at the Huaniao Isle, very close to that in heavy fuel oil used by domestic ships (Zhao et al., 2013a), which further corroborated the characteristics of ship emission origin over the remote East China Sea.

3.3. Impact of the long/medium-range transport on the heavy haze formation

Fig. 8 shows the 48-h air masses backward trajectories ending in Shanghai, Beijing, and the Huaniao Isle, respectively, during the severely polluted days. In Shanghai (Fig. 8a), the air masses during PD_SH were mainly limited within the YRD region, e.g. Jiangsu and Zhejiang provinces and occasionally extended to Shandong province. This type of transport is referred as the medium-range transport. The ratio of NO_3^-/SO_4^{2-} was in the range of 1.1–2.0 during Jan. 12–15, close to that (1.2) of the previous studies on the haze occurred over Shanghai, in which the haze was dominated by local and YRD emissions (Huang et al., 2013b). On Jan. 16, the backward trajectories starting from Shanghai traced back to the North China Plain. This was corroborated by a significant drop of the ratio of NO_3^-/SO_4^{2-} to be 0.6, which was close to that observed in Beijing, confirming the impact of the long-range transport from Northern China on the severe haze formation in Shanghai, the downstream regions of the transport. The Potential Source Contribution Function (PSCF, see Appendix in Supplementary Materials) facilitated a more clear visualization of the extent of transport. Based on the hourly $PM_{2.5}$ concentrations at one SEMC (Shanghai Environmental Monitoring Center) site (Yangpu Sipiao, about 5 km from our sampling site) during Jan. 12–15, 2013, weighted PSCF is plotted in Fig. 8b. It is clearly shown that the potential source regions of particulate pollution in Shanghai were constrained in limited areas. Local Shanghai, the southern tip of Jiangsu province and the northern tip of Zhejiang province showed relatively high PSCF values. It is noted that there were also high probabilities of drifting from the north over the East China Sea. This was likely the continental outflow from Jiangsu province and indicated that the high particulate pollution of Shanghai was partly ascribed to regional transport.

In Beijing, the air masses on Jan. 10 and Jan. 12–13 mostly travelled through Beijing at low altitudes and passed over those neighboring areas around Beijing with intense emission rates, such as Hebei, Shanxi provinces and Tianjin (Fig. 8c). For example, on Jan. 12 which was the severest pollution day, SO_4^{2-} increased 92% as compared to Jan. 11, while NO_3^- increased ~51%, resulting in a ratio of $\Delta NO_3^-/\Delta SO_4^{2-}$ of as low as 0.4. Based on the emission inventory data (Zhao et al., 2012), the emission rate ratio of NO_x/SO_2 of Beijing was more than 1.5, while the emission rate of SO_2 was almost twice of NO_x for the entire North China Plain. The measured NO_3^-/SO_4^{2-} ratio in aerosol of Beijing was more consistent with the NO_x/SO_2 emission rate ratio of the North China Plain rather than Beijing

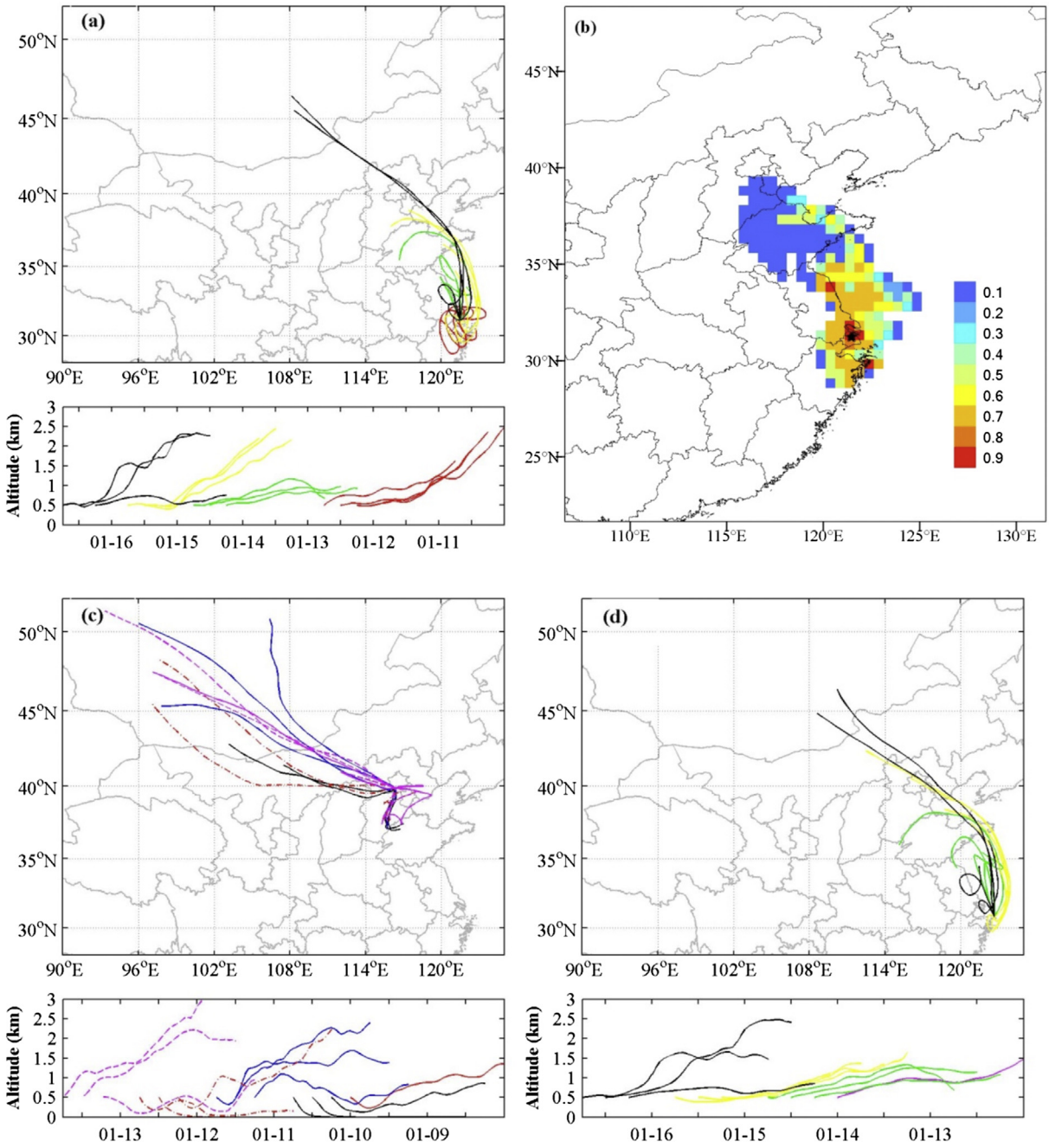

Fig. 8. (a) 48 h back trajectories of air masses in PD_SH. (b) The potential source contribution function (PSCF) map for $PM_{2.5}$ in Shanghai during Jan. 12–15, 2013. The monitoring site at Shanghai is denoted by the black star in figure. (c) 48 h back trajectories of air masses in PD_BJ. (d) 48 h back trajectories of air masses in PD_HN.

itself, implying a significant contribution from regional transport to the haze formation over Beijing. Other evidences were also indicated that those coal-related species such as Cl^-, As, Cd, and Pb all increased more than 80% on Jan. 12 as compared to Jan. 11.

As for the Huaniao Isle, the backward trajectories indicated that the aerosol during PD_HN could be impacted by emissions from Northern China as well as the YRD region (Fig. 8d). On one hand, the local anthropogenic emissions were negligible at the Huaniao Isle. On the other hand, temperature during this period was low and should significantly suppress the evaporation of nitrate. Hence, the NO_3^-/SO_4^{2-} ratio could be regarded as a good tracer for identifying the source region. As shown in Table 2, the NO_3^-/SO_4^{2-} ratio at the Huaniao Isle during the normal days showed the lowest values of 0.4 among all three sites. The average NO_3^- concentration at this isle was as low as 1.3 μg m^{-3}, which could be regarded as the background concentration of NO_3^- over China. The Huaniao Isle has less than 2500 local residents with very few on-road transportation tools. Shipping emission was probably a major source of NO_3^-. Hence, the low NO_3^-/SO_4^{2-} ratio during ND_HN was expected. In PD_HN, the NO_3^-/SO_4^{2-} ratio was elevated to 0.6. Unexpectedly, the NO_3^-/SO_4^{2-} ratio of the Huaniao Isle was fairly close to that of Beijing rather than that of the adjacent Shanghai. The very similar ratio of NO_3^-/SO_4^{2-} between the Huaniao Isle and Beijing suggested that the impact from Northern China on the remote East China Sea via long-range transport had significantly overwhelmed the regional impact from the YRD region. Additional

Table 2
Concentrations of SO_4^{2-} and NO_3^- and the ratios of NO_3^-/SO_4^{2-} in $PM_{2.5}$ from this study and the previous studies.

Sites	Observation time	SO_4^{2-}	NO_3^-	NO_3^-/SO_4^{2-}	Reference
Shanghai	1999–2000 Annual	15.2	6.5	0.4	Yao et al. (2002)
	2005 Winter	15.8	7.1	0.5	Wang et al. (2006)
	2006 Winter	9.6	6.8	0.7	Fu et al. (2008)
	2010 Spring-fall	6.5	7.5	1.2	Huang et al. (2013)
	2012 Winter ND	9.2	9.2	1.0	This study
	2012 Winter PD	25.7	37.3	1.4	This study
Beijing	1999–2000 Annual	17.7	10.1	0.6	Yao et al. (2002)
	2001–2003 Winter	21.0	12.3	0.58	Wang et al. (2005)
	2004 Winter Haze	29.5	17.1	0.58	Sun et al. (2006)
	2013 Jan. EP1	30.6	22.0	0.72	Sun et al. (2014)
	2013 Jan. EP2	24.8	19.5	0.78	Sun et al. (2014)
	2013 Jan. EP3	65.3	40.2	0.62	Sun et al. (2014)
	2013 Jan. EP4	32.0	23.1	0.72	Sun et al. (2014)
	2013 Jan. ND	4.6	3.8	0.83	This study
	2013 Jan. PD	56.1	34.9	0.62	This study
Huaniao Isle	2012 Winter ND	4.4	1.3	0.4	This study
	2012 Winter PD	19.5	11.8	0.6	This study

ND: normal days.
PD: severely polluted days.

evidences were revealed by comparing the ratios of pollution elements, As, Cd, Cu, Zn and water-soluble ion, K^+ to Al among the three sites (Table 3). These tracer ratios in ND_HN were more close to those in Shanghai, indicating the dominant impacts from YRD on the remote East China Sea when the long-range transport effect was minimal. While during PD_HN in this study, all the tracer ratios were elevated and approached closer to those of Beijing (PD_BJ) rather than Shanghai (PD_SH), which was likely the result of mixing of the regional emissions and the long-range transported pollutants. Specifically, the ratios of Cd/Al, Cu/Al, Zn/Al in PD_HN were evidently more close to those of PD_BJ while much higher than those of PD_SH. In contrast, the ratios of K^+/Al and As/Al in PD_HN were about half of those in PD_BJ although they were higher than those in ND_HN. It should be noted that Cd, Cu, Zn were mainly characterized of industrial sources. In China, industries were densely distributed over large areas. Hence, the trajectories that passed over Northern China were likely representative. As for K^+ which is a typical tracer for biomass burning, its spatial distribution should be much more random than the industrial sources as it depended on the fire locations. It was possible that the trajectories didn't intercept the major biomass burning areas in Northern China and thus the K^+/Al ratio in PD_HN was much lower than that in PD_BJ. Also for As which is a tracer for coal-fired power plants, the density of power plants is also smaller than the industries. Hence, it was also possible that the backward trajectories that intercepted Northern China were not representative of the areas around the sampling site in Beijing. Overall, it was found that the plumes that invaded the Huaniao Isle were well characterized of origin from Northern China via the long-range transport.

3.4. Stationary vs. mobile sources in the megacities

The mass ratio of NO_3^-/SO_4^{2-} in aerosol was suggested as an indicator of the relative contribution of mobile vs. stationary sources (Arimoto et al., 1996). High NO_3^-/SO_4^{2-} ratios were observed in those areas where traffic emission is the dominant anthropogenic source. For instance, the ratio could reach as high as 2.0 in Los Angeles, USA (Gao et al., 1996). In this study, we also calculated the mean ratios of NO_3^-/SO_4^{2-} in $PM_{2.5}$ during ND and PD at the three sites and compared to the values from previous studies (Fu et al., 2008; Huang et al., 2013a; Wang et al., 2005; Wang et al., 2006; Yao et al., 2002). The results are shown in Table 2. In Shanghai, the ratio of NO_3^-/SO_4^{2-} reached 1.0 during ND_SH and 1.4 during PD_SH, much higher than that during PD_BJ and ND_BJ (Table 2). In the long-term, the ratio of NO_3^-/SO_4^{2-} in Shanghai increased quickly from 0.4 to 0.7 before 2007 to more than 1.0 after 2010. Consistently, the ratio of ambient NO_2/SO_2 increased from ~1.0 in 2005 to 2.0 in 2012 (Shanghai Statistical Yearbook, 2006–2013). The annual average concentrations of SO_2 over Shanghai significantly decreased ~60% from 61 μg m^{-3} in 2005 to 23 μg m^{-3} in 2012 (Shanghai Statistical Yearbook, 2006–2013). On the other hand, the retain number of vehicles sharply increased from around 1 million in 2000 to 3.3 million in 2011 (Shanghai Statistical Yearbook, 2002–2012). Thus, the ambient concentration of NO_2 decreased much slower than SO_2 with a moderate reduction of 25% from 61 μg m^{-3} in 2005 to 46 μg m^{-3} in 2012 (Shanghai Statistical Yearbook, 2006–2013). Hence, the increasing motor vehicle emission in Shanghai could explain the increasing trend of NO_3^-/SO_4^{2-} observed in aerosol. This suggested that the traffic emission had become a more important source for the formation of the severe haze.

In Beijing, during the winter of 2001–2003 and a haze-fog episode in the winter of 2004, the mass ratio of NO_3^-/SO_4^{2-} was at the relatively low level of 0.58 (Wang et al., 2005; Sun et al., 2006). In 2013, the average ratio of NO_3^-/SO_4^{2-} during ND_BJ was 0.83, suggesting that the relative contributions of stationary source vs. mobile source in Beijing had greatly changed. This was mainly due to that the stationary sources such as coal-fired power

Table 3
Average ratios of K^+, As, Cd, Cu, and Zn to Al in normal days and in the severely polluted days.

	ND_BJ	PD_BJ	ND_SH	PD_SH	ND_HN	PD_HN
K^+/Al	0.8 ± 0.7	9.0 ± 1.6	3.0 ± 0.7	2.7 ± 0.3	1.2 ± 1.5	5.3 ± 1.5
As/Al	(1.8 ± 2.6)*10^{-2}	(9.3 ± 2.5)*10^{-2}	(3.1 ± 1.6)*10^{-2}	(3.2 ± 0.2)*10^{-2}	(3.3 ± 2.9)*10^{-2}	(4.5 ± 1.5)*10^{-2}
Cd/Al	(9.9 ± 8.0)*10^{-4}	(8.2 ± 1.3)*10^{-3}	(1.6 ± 0.6)*10^{-3}	(3.4 ± 1.9)*10^{-3}	(4.2 ± 3.0)*10^{-3}	(1.1 ± 0.4)*10^{-2}
Cu/Al	(2.2 ± 2.0)*10^{-2}	(9.9 ± 1.8)*10^{-2}	(3.7 ± 1.0)*10^{-2}	(4.8 ± 1.1)*10^{-2}	(5.0 ± 3.6)*10^{-2}	(8.6 ± 3.4)*10^{-2}
Zn/Al	0.2 ± 0.2	1.3 ± 0.3	0.5 ± 0.1	0.7 ± 0.2	0.5 ± 0.4	1.0 ± 0.3

plants and steel/cement industries in Beijing had been largely reduced in recently years. In contrast, during PD_BJ, the ratio of NO_3^-/SO_4^{2-} was much lower of 0.62. As shown in Table 2, Sun et al. (2014) found the ratios of NO_3^-/SO_4^{2-} ranged from 0.62 to 0.78 during different pollution episodes in Beijing in January, 2013. Considering that the study by Sun et al. (2014) measured PM_1 and their sampling site is around 18 km from ours, their results were comparable to this study. It seemed that the ratio of NO_3^-/SO_4^{2-} during the polluted episode did not vary significantly, as compared to the early years. The coal combustion and traffic emission were two of the dominated sources in this severe haze over Beijing. It must be noted that the aerosol over a city was not only from the local emission but also from the long- or medium-range transport as discussed above. The regional transport contributed quite a lot to the aerosol over Beijing. As for SO_2 and its oxidation product sulfate, coal-fired power plants and steel/cement industries are their major emission sources. For example, Hebei province that surrounds the whole Beijing produced over 1/3 of the steel of the entire China in recent years and the coal consumption increased 34% from 546,882 tons of standard coal equivalent (SCE) per day in 2006 to 735,958 tons of SCE per day in 2012 (Hebei Economic Yearbook, 2007–2013). It was reported that the annual average ratio of NO_2/SO_2 was in low levels of 0.5–0.7 in Hebei (Hebei Province Environment Condition Bulletin, 2007–2013). This meant that the SO_4^{2-} produced in Hebei should be much greater than NO_3^-. Thus, if the great part of SO_4^{2-} from the regional transport to Beijing was considered, the ratio of NO_3^-/SO_4^{2-} in the severely polluted days in January 2013 in Beijing should be lower than 0.58 as compared to that in the 2001–2004 (Table 2). However, this ratio of NO_3^-/SO_4^{2-} in this heavy haze episode was not lower than that of ten years ago, instead, it was as high as 0.62. This meant that while SO_4^{2-} increased, NO_3^- in the aerosol increased even more than SO_4^{2-} did in this severe haze episode. The traffic exhaust is one of the major sources of NO_x and the number of vehicles in Beijing increased rapidly from ~1.4 million in 2000 to ~5.2 million in 2012 (Beijing Statistical Yearbook, 2001–2013), thus, the increased NO_3^- could be more attributed to the traffic emission. According to the source apportionment results (Beijing EPB, 2014), even without considering the regional transport, the contribution from local traffic emission to $PM_{2.5}$ in Beijing was over 30%. The combining evidence indicated that the traffic emission has also been one of the major sources in triggering the severe haze formation in Beijing.

4. Conclusion

An extremely severe haze shrouded over northern and eastern China in Jan. 1–19, 2013, which even extended to those remote areas over the East China Sea. Considering the high relative humidity conditions during the severely polluted days, this work suggests that the promoted gas-to-particle transformations from acidic SO_2 and NO_x to SO_4^{2-} and NO_3^- play a major role in the formation of this severe haze. Significant contribution of traffic emissions to the haze formation over China was suggested to be one of the major sources in triggering the heavy haze over China. The much higher NO_3^-/SO_4^{2-} ratio in Shanghai suggest a more significant contribution of traffic emissions to the haze formation than in Beijing where coal combustion and traffic emissions were two of the major contributors in triggering the haze. However, traffic emission was still an important contributor to this heavy haze in Beijing during some specific episodes (Wang et al., 2014c).

Impacts of the long/medium-range transport on the formation of this severe haze were significant, as indicated in the remote site, the Huaniao Isle. The substantial increases of pollution elements, secondary ions, and K^+ during the severely polluted days were attributed to the transport of air pollutants. The ratios of As, Cd, Cu, Zn, and K^+ to Al at the Huaniao Isle were much more close to the ratios in Beijing rather than in Shanghai, indicating that the marine aerosol over the East China Sea had been significantly polluted by the long-range transport of anthropogenic pollutants originating from Northern China.

Acknowledgment

This work was supported by National Natural Science Foundation of China (Grant Nos. 21277030, 41429501 (fund for collaboration with overseas scholars), and 41405115), Environmental charity project of Ministry of Environmental Protection of China (201409022), and the open project of Shanghai key laboratory of atmospheric particle pollution prevention (FDLAP13005).

Appendix A. Supplementary data

Supplementary data related to this article can be found at http://dx.doi.org/10.1016/j.atmosenv.2015.08.076.

References

An, J.L., Li, Y., Chen, Y., Li, J., Qu, Y., Tang, Y.J., 2013. Enhancements of major aerosol components due to additional HONO sources in the North China Plain and implications for visibility and haze. Adv. Atmos. Sci. 30 (1), 57–66. http://dx.doi.org/10.1007/s00376-012-2016-9.

Andreae, M.O., 1983. Soot carbon and excess fine potassium: long-range transport of combustion-derived aerosols. Sci. (New York, NY) 220, 1148.

Arimoto, R., Duce, R.A., Savoie, D.L., Prospero, J.M., Talbot, R., Cullen, J.D., Tomza, U., Lewis, N.F., Ray, B.J., 1996. Relationships among aerosol constituents from Asia and the North Pacific during PEM-West A. J. Geophys. Res. Atmos. 101, 2011–2023.

Beijing EPB, 2014. Environmental Protection Bureau (in Chinese). http://tech.sina.com.cn/d/2014-10-31/14329750274.shtml.

Beijing Statistical Yearbook, 2001–2013. China Statistics Press, Beijing.

Chen, L.W.A., Chow, J.C., Doddridge, B.G., Dickerson, R.R., Ryan, W.F., Mueller, P.K., 2003. Analysis of a summertim PM2.5 and haze episode in the mid-Atlantic region. J. Air Waste Manag. Assoc. 53, 946–956.

Cheng, M.C., You, C.F., Cao, J., Jin, Z., 2012. Spatial and seasonal variability of water-soluble ions in PM2.5 aerosols in 14 major cities in China. Atmos. Environ. 60, 182–192.

Cheng, Z., Wang, S., Fu, X., Watson, J.G., Jiang, J., Fu, Q., Chen, C., Xu, B., Yu, J., Chow, J.C., Hao, J., 2014. Impact of biomass burning on haze pollution in the Yangtze River delta, China: a case study in summer 2011. Atmos. Chem. Phys. 14, 4573–4585.

Duan, J.C., Tan, J.H., 2013. Atmospheric heavy metals and arsenic in China: situation, sources and control policies. Atmos. Environ. 74, 93–101.

Fu, Q.Y., Zhuang, G.S., Wang, J., Xu, C., Huang, K., Li, J., Hou, B., Lu, T., Streets, D.G., 2008. Mechanism of formation of the heaviest pollution episode ever recorded in the Yangtze River Delta, China. Atmos. Environ. 42, 2023–2036.

Gao, Y., Arimoto, R., Duce, R.A., Chen, L.Q., Zhou, M.Y., Gu, D.Y., 1996. Atmospheric non-sea-salt sulfate, nitrate and methanesulfonate over the China Sea. J. Geophys. Res. Atmos. 101, 12601–12611.

Guo, L., Chen, Y., Wang, F.J., Meng, X., Xu, Z.F., Zhuang, G.S., 2014. Effects of Asian dust on the atmospheric input of trace elements to the East China Sea. Mar. Chem. 163, 19–27.

Hebei Economic Yearbook, 2007–2013. China Statistics Press, Beijing.

Hebei Province Environment Condition Bulletin, 2007-2013. Hebei Provincial Environmental Protection Hall. http://www.hb12369.net/hjzlzkgb/.

Hsu, S.C., Liu, S.C., Huang, Y.T., Chou, C.C.K., Lung, S.C.C., Liu, T.H., Tu, J.Y., Tsai, F.J., 2009. Long-range southeastward transport of Asian biosmoke pollution: signature detected by aerosol potassium in Northern Taiwan. J. Geophys. Res. Atmos. 114.

Huang, K., Zhuang, G., Lin, Y., Fu, J.S., Wang, Q., Liu, T., Zhang, R., Jiang, Y., Deng, C., Fu, Q., Hsu, N.C., Cao, B., 2012. Typical types and formation mechanisms of haze in an Eastern Asia megacity. Shanghai. Atmos. Chem. Phys. 12, 105–124.

Huang, K., Zhuang, G., Lin, Y., Wang, Q., Fu, J.S., Fu, Q., Liu, T., Deng, C., 2013a. How to improve the air quality over mega-cities in China? – pollution characterization and source analysis in Shanghai before, during, and after the 2010 World Expo. Atmos. Chem. Phys. Discuss. 13, 3379–3418.

Huang, K., Zhuang, G., Lin, Y., Wang, Q., Fu, J.S., Fu, Q., Liu, T., Deng, C., 2013b. How to improve the air quality over megacities in China: pollution characterization and source analysis in Shanghai before, during, and after the 2010 World Expo. Atmos. Chem. Phys. 13, 5927–5942.

Huang, K., Zhuang, G., Wang, Q., Fu, J.S., Lin, Y., Liu, T., Han, L., Deng, C., 2014. Extreme haze pollution in Beijing during January 2013: chemical characteristics, formation mechanism and role of fog processing. Atmos. Chem. Phys. Discuss. 14, 7517–7556.

Jacobson, M.Z., 1997. Development and application of a new air pollution modeling system .2. Aerosol module structure and design. Atmos. Environ. 31, 131–144.
Ji, D., Li, L., Wang, Y., Zhang, J., Cheng, M., Sun, Y., Liu, Z., Wang, L., Tang, G., Hu, B., Chao, N., Wen, T., Miao, H., 2014. The heaviest particulate air-pollution episodes occurred in northern China in January, 2013: insights gained from observation. Atmos. Environ. 92, 546–556.
Kang, C.M., Lee, H.S., Kang, B.W., Lee, S.K., Sunwoo, Y., 2004. Chemical characteristics of acidic gas pollutants and PM2.5 species during hazy episodes in Seoul, South Korea. Atmos. Environ. 38, 4749–4760.
Lang, J.L., Cheng, S.Y., Wei, W., Zhou, Y., Wei, X., Chen, D.S., 2012. A study on the trends of vehicular emissions in the Beijing-Tianjin-Hebei (BTH) region, China. Atmos. Environ. 62, 605–614.
Li, Y., An, J.L., Gultepe, I., 2014. Effects of additional HONO sources on visibility over the North China Plain. Adv. Atmos. Sci. 31 (5), 1221–1232. http://dx.doi.org/10.1007/s00376-014-4019-1.
Lida, D.R., 2006. Handbook of Chemistry and Physics: a Ready-Reference Book of Chemical and Physical Data, 86th ed. CRC Press, New York, pp. 14–17.
Lin, Y., Huang, K., Zhuang, G., Fu, J., Xu, C., Shen, J., Chen, S., 2013. Air quality over the Yangtze River Delta during the 2010 Shanghai expo. Aerosol Air Qual. Res. 13, 1655–1666.
Meng, Y.J., Wang, S.Y., Zhao, X.F., 2000. An analysis of air pollution and weather conditions during heavy fog days in Beijing area (in Chinese). Weather 26.
Menon, S., Hansen, J., Nazarenko, L., Luo, Y.F., 2002. Climate effects of black carbon aerosols in China and India. Science 297, 2250–2253.
Mestl, H.E.S., Aunan, K., Seip, H.M., Wang, S., Zhao, Y., Zhang, D., 2007. Urban and rural exposure to indoor air pollution from domestic biomass and coal burning across China. Sci. Total Environ. 377, 12–26.
Shanghai Statistical Yearbook, 2002-2013. China Statistics Press, Beijing.
Sun, Y.L., Jiang, Q., Wang, Z.F., Fu, P.Q., Li, J., Yang, T., Yin, Y., 2014. Investigation of the sources and evolution processes of severe haze pollution in Beijing in January 2013. J. Geophys. Res. Atmos. 119, 4380–4398.
Sun, Y.L., Wang, Z.F., Fu, P.Q., Jiang, Q., Yang, T., Li, J., Ge, X.L., 2013a. The impact of relative humidity on aerosol composition and evolution processes during wintertime in Beijing, China. Atmos. Environ. 77, 927–934.
Sun, Y.L., Wang, Z.F., Fu, P.Q., Yang, T., Jiang, Q., Dong, H.B., Li, J., Jia, J.J., 2013b. Aerosol composition, sources and processes during wintertime in Beijing, China. Atmos. Chem. Phys. 13, 4577–4592.
Sun, Y.L., Zhuang, G.S., Tang, A.H., Wang, Y., An, Z.S., 2006. Chemical characteristics of PM2.5 and PM10 in haze-fog episodes in Beijing. Environ. Sci. Technol. 40, 3148–3155.
Sun, Y.L., Zhuang, G.S., Ying, W., Han, L.H., Guo, J.H., Mo, D., Zhang, W.J., Wang, Z.F., Hao, Z.P., 2004. The air-borne particulate pollution in Beijing – concentration, composition, distribution and sources. Atmos. Environ. 38, 5991–6004.
Takuwa, T., Mkilaha, I.S.N., Naruse, I., 2006. Mechanisms of fine particulates formation with alkali metal compounds during coal combustion. Fuel 85, 671–678.
Tan, J.H., Duan, J.C., Chen, D.H., Wang, X.H., Guo, S.J., Bi, X.H., Sheng, G.Y., He, K.B., Fu, J.M., 2009. Chemical characteristics of haze during summer and winter in Guangzhou. Atmos. Res. 94, 238–245.
Tanner, P.A., Ma, H.-L., Yu, P.K.N., 2008. Fingerprinting metals in urban street dust of Beijing, Shanghai, and Hong Kong. Environ. Sci. Technol. 42, 7111–7117.
Tian, H., Cheng, K., Wang, Y., Zhao, D., Lu, L., Jia, W., Hao, J., 2012. Temporal and spatial variation characteristics of atmospheric emissions of Cd, Cr, and Pb from coal in China. Atmos. Environ. 50, 157–163.
Tian, H.Z., Wang, Y., Xue, Z.G., Cheng, K., Qu, Y.P., Chai, F.H., Hao, J.M., 2010. Trend and characteristics of atmospheric emissions of Hg, As, and Se from coal combustion in China, 1980–2007. Atmos. Chem. Phys. 10, 11905–11919.
Wang, H., An, J., Shen, L., Zhu, B., Pan, C., Liu, Z., Liu, X., Duan, Q., Liu, X., Wang, Y., 2014a. Mechanism for the formation and microphysical characteristics of submicron aerosol during heavy haze pollution episode in the Yangtze River Delta, China. Sci. Total Environ. 490, 501–508.
Wang, L.T., Wei, Z., Yang, J., Zhang, Y., Zhang, F.F., Su, J., Meng, C.C., Zhang, Q., 2014b. The 2013 severe haze over southern Hebei, China: model evaluation, source apportionment, and policy implications. Atmos. Chem. Phys. 14, 3151–3173.
Wang, Y., Zhuang, G.S., Tang, A.H., Yuan, H., Sun, Y.L., Chen, S.A., Zheng, A.H., 2005. The ion chemistry and the source of PM2.5 aerosol in Beijing. Atmos. Environ. 39, 3771–3784.
Wang, Y., Zhuang, G.S., Zhang, X.Y., Huang, K., Xu, C., Tang, A.H., Chen, J.M., An, Z.S., 2006. The ion chemistry, seasonal cycle, and sources of PM2.5 and TSP aerosol in Shanghai. Atmos. Environ. 40, 2935–2952.
Wang, Y.S., Yao, L., Wang, L.L., Liu, Z.R., Ji, D.S., Tang, G.Q., Zhang, J.K., Sun, Y., Hu, B., Xin, J.Y., 2014c. Mechanism for the formation of the January 2013 heavy haze pollution episode over central and eastern China. Sci. China Earth Sci. 57, 14–25.
Wang, Z.F., Li, J., Wang, Z., Yang, W.Y., Tang, X., Ge, B.Z., Yan, P.Z., Zhu, L.L., Chen, X.S., Chen, H.S., Wang, W., Li, J.J., Liu, B., Wang, X.Y., Wang, W., Zhao, Y.L., Lu, N., Su, D., 2014d. Modeling study of regional severe hazes over mid-eastern China in January 2013 and its implications on pollution prevention and control. Sci. China Earth Sci. 57, 3–13.
Yang, D.-q., Kwan, S.H., Lu, T., Fu, Q.-y., Cheng, J.-m., Streets, D.G., Wu, Y.-m., Li, J.-j., 2007. An emission inventory of marine vessels in shanghai in 2003. Environ. Sci. Technol. 41, 5183–5190.
Yao, X., Chan, C.K., Fang, M., Cadle, S., Chan, T., Mulawa, P., He, K., Ye, B., 2002. The water-soluble ionic composition of PM2.5 in Shanghai and Beijing, China. Atmos. Environ. 36, 4223–4234.
Yuan, H., Wang, Y., Zhuang, G., 2003. The simultaneous determination of organic acid, MSA with inorganic anions in aerosol and rainwater by ion chromatography (in Chinese). J. Instrum. Analysis 6, 6–12.
Zhang, R.H., Li, Q., Zhang, R.N., 2014a. Meteorological conditions for the persistent severe fog and haze event over eastern China in January 2013. Sci. China Earth Sci. 57, 26–35.
Zhang, Z.L., Wang, J., Chen, L.H., Chen, X.Y., Sun, G.Y., Zhong, N.S., Kan, H.D., Lu, W.J., 2014b. Impact of haze and air pollution-related hazards on hospital admissions in Guangzhou, China. Environ. Sci. Pollut. Res. 21, 4236–4244.
Zhao, B.A., Wang, P.A., Ma, J.Z.A., Zhu, S.A., Pozzer, A.A., Li, W.T., 2012. A high-resolution emission inventory of primary pollutants for the Huabei region, China. Atmos. Chem. Phys. 12, 481–501.
Zhao, M., Zhang, Y., Ma, W., Fu, Q., Yang, X., Li, C., Zhou, B., Yu, Q., Chen, L., 2013a. Characteristics and ship traffic source identification of air pollutants in China's largest port. Atmos. Environ. 64, 277–286.
Zhao, P.S., Dong, F., He, D., Zhao, X.J., Zhang, X.L., Zhang, W.Z., Yao, Q., Liu, H.Y., 2013b. Characteristics of concentrations and chemical compositions for PM2.5 in the region of Beijing, Tianjin, and Hebei, China. Atmos. Chem. Phys. 13, 4631–4644.
Zhao, X.J., Zhao, P.S., Xu, J., Meng, W., Pu, W.W., Dong, F., He, D., Shi, Q.F., 2013c. Analysis of a winter regional haze event and its formation mechanism in the North China Plain. Atmos. Chem. Phys. 13, 5685–5696.
Zhu, T., Shang, J., Zhao, D.F., 2010. The roles of heteorogeneous chemical processes in the formation of an air pollution complex and gray haze. Sci. Sin. Chim. 40 (12), 1731–1740 (in Chinese).